UDC 621.319 https://doi.org/10.20998/2074-272X.2026.1.10

G.V. Bezprozvannych, I.A. Pushkar

Influence of gamma radiation on the electrical and mechanical properties of on-board systems cables

Introduction. *Electrical and fiber-optic cables of on-board systems for transmitting monitoring, control and communication signals are increasingly used in nuclear power plants, aircraft systems and military applications. Such operating conditions are characterized by an increased level of ionizing radiation compared to the background: from 10 kGy in space applications to 1 GGy in the corium of a nuclear reactor.* ***Problem.*** *The resistance of polymer insulation to the action of ionizing radiation is determined on the basis of mechanical, thermophysical, physicochemical indicators that reflect the local characteristics of the polymer insulation of electrical cables. Modern special radiation-resistant optical fibers are capable of operating under the action of gamma radiation with a dose of 1 MGy. To ensure mechanical strength and protection of the optical fiber from moisture, high-strength structural elements and hydrophobic fillers are used in the optical cable. The* ***goal*** *of the work consists in establishing the effect of gamma radiation on unshielded cables with unshielded twisted pairs and optical cables with the determination of the dynamics of changes in the electrical properties of polyethylene insulation of conductors and mechanical properties of aramid yarns with a water-blocking coating, respectively.* ***Methodology*** *is based on the determination of the change in the electrical capacitance of each of the 8 polyethylene-insulated twisted pair conductors and the mechanical tensile strength of Kevlar yarns with a water-blocking compound, compared to the un-irradiated state, depending on the absorbed dose of gamma radiation of 100 kGy, 200 kGy and 300 kGy when processing samples of electrical and optical cables in the cobalt-60 (Co^{60}) installation.* ***Scientific novelty*** *consists in establishing the criterion for achieving the critical state of polymeric polyethylene insulation of insulated conductors and the effect of the influence of a water-blocking coating with ultra-high absorption capacity on the mechanical strength of aramid yarns under the action of gamma radiation on samples of an electric cable in a protective sheath of polyvinyl chloride plastic compound and an optical cable in a protective sheath based on a polymer fire-resistant composition, respectively.* ***Practical value*** *is qualified by the range of radiation resistance of structural elements to ensure the operational functionality and efficiency of cables of on-board systems under the action of gamma radiation.* References 50, tables 3, figures 6.

Key words: **on-board systems, unshielded cable with unshielded twisted pairs, optical cable, absorbed dose of gamma radiation, polyethylene insulation, electrical capacitance, aramid yarns, waterproof compound, mechanical tensile strength, radiation resistance.**

Вступ. *Електричні та оптичні кабелі бортових систем для передачі сигналів моніторингу, керування та зв'язку все частіше використовуються на атомних електричних станціях, в системах літальних апаратів та військовому застосуванні. Такі умови експлуатації характеризуються підвищеним порівняно з фоновим рівнем іонізуючого випромінювання: від 10 кГр у космічних застосуваннях до 1 ГГр в активній зоні ядерного реактора.* ***Проблема****. Стійкість полімерної ізоляції до дії іонізуючого випромінювання визначається на підставі механічних, теплофізичних, фізико-хімічних показників, які відображають локальні характеристики полімерної ізоляції електричних кабелів. Сучасні спеціальні радіаційно-стійкі оптичні волокна здатні працювати при дії гамма-випромінення дози 1 МГр. Задля забезпечення механічної міцності та захисту від вологи оптичного волокна в оптичному кабелі застосовуються високоміцні конструктивні елементи та гідрофобні заповнювачі.* ***Мета*** *роботи полягає у встановленні впливу гамма-випромінення на неекрановані кабелі з неекранованими витими парами та оптичні кабелі з визначенням динаміки змінення електричних властивостей поліетиленової ізоляції провідників та механічних властивостей арамідних ниток з водозахисним покриттям відповідно.* ***Методика*** *ґрунтується на визначенні порівняно з неопроміненим станом змінення електричної ємності кожного з восьми ізольованих поліетиленом провідників витих пар та механічної міцності на розтяг кевларових ниток з водозахисним компаундом в залежності від поглиненої дози гамма-випромінення 100 кГр, 200 кГр та 300 кГр при обробці зразків електричного та оптичного кабелів в установці кобальт-60 (Co^{60}).* ***Наукова новизна*** *полягає у встановленні критерію досягнення критичного стану полімерної поліетиленової ізоляції ізольованих провідників та ефекту впливу водозахисного покриття з надвисокою поглинальною здатністю на механічну міцність арамідних ниток при дії гамма-випромінення на зразки електричного кабелю у захисній полімерній оболонці з поліхлорвінілового пластику та оптичного кабелю у захисній оболонці на основі полімерної вогнестійкої композиції відповідно.* ***Практична цінність*** *кваліфікується діапазоном радіаційної стійкості конструктивних елементів для забезпечення експлуатаційної функціональності та ефективності кабелів бортових систем в умовах дії гамма-випромінення.* Бібл. 50, табл. 3, рис. 6.

Ключові слова: **бортові системи, неекранований кабель з неекранованими витими парами, оптичний кабель, поглинена доза гамма-випромінення, поліетиленова ізоляція, електрична ємність, арамідні нитки, водозахисний компаунд, механічна міцність на розтяг, радіаційна стійкість.**

Introduction. As critical safety components, on-board cables play a crucial role in connecting various electronic and electrical systems, including radar systems, avionics, navigation equipment, and weapons systems [1–10]. The main purpose of on-board cables is to collect and manage data; distribute power with simultaneous data transmission; and provide reliable and secure communication with a high level of noise immunity. Twisted pair and optical cables are increasingly used for real-time transmission of monitoring, control, data, and communication signals in on-board systems and nuclear power plants (NPPs) [1–14].

The trend towards miniaturization continues to affect all aspects of on-board systems. Innovations in electrical insulation materials and cable designs make this possible without sacrificing system performance by creating hybrid cables by combining electrical and optical in a single design.

Cables must meet a list of requirements related to functional characteristics, dimensions, and weight. The operational functionality of cables in on-board systems is determined by their resistance to the influence of external and internal factors. The first ones include such operating conditions of cables as temperature, pressure, air humidity, the presence of external tensile mechanical loads [10], chemical aggressiveness of the external environment and the influence of radiation [12]. The operation of cables of on-board systems is characterized by an increased level of ionizing radiation compared to the background. Thus, at a NPP under normal operating conditions at elevated temperature, cables of the sealed zone are constantly exposed to gamma radiation [13–17]. Outside the radiation protection of the reactor, the radiation level approaches the background, and the temperature approaches the ambient temperature. Aerospace cables [12] are exposed to solar radiation, including intense solar flares. Military cables (aircraft, unmanned aerial vehicles) can also be exposed to natural and artificial radiation, including nuclear explosions [1, 7]. Radiation levels can range from 10 kGy when using cables in space applications to 1 GGy in the core of a nuclear reactor [17–19].

Problem definition. Ionizing energy sources (absorbed dose) fully determine the full effect of exposure to polymers used as electrical insulation of cables and optical quartz fibers [20–31].

The following main processes occur in polymers when exposed to ionizing radiation:

- creation of chemical bonds, both between and within macromolecules, destruction and decomposition of macromolecules with the release of gaseous and liquid components, change in the number and nature of double bonds (in the presence of oxygen) and other processes [23–27];
- long chains can connect into rigid three-dimensional networks (crosslinking process) or split into smaller molecules (destruction process). Both processes can occur simultaneously, so at a certain absorbed radiation dose, the final properties and structure of the polymer will be determined by the reaction that dominates [23–27].

For polyethylene, as the absorbed radiation dose increases, the degree of crosslinking increases and, at the same time, fragments of molecular decay accumulate, which in aggregate leads to a decrease in mechanical properties and material destruction [25, 26]. Radiation destruction of macromolecules leads to a decrease in mechanical strength, an increase (up to a certain limit) in relative elongation, and cracking. The polymer surface becomes sticky. The dose required for crosslinking polyethylene is (200–400) kGy [28, 29]. The radiation resistance of polyvinyl chloride plastic is determined by the permissible absorbed dose of gamma radiation at the level of 500 kGy [28] and is established, as for many other polymer materials, on the basis of mechanical, thermophysical, and physicochemical parameters [28–32]. These indicators reflect the indirect characteristics of polymer insulation, unlike electrical ones, which are basic and have an integral nature and reflect the state of cable insulation as a whole.

In optical cables, the effect of radiation separately on optical fibers is considered to the greatest extent [33–36]. Quartz optical fibers are characterized by higher values of the radiation dose at which structural damage occurs, compared to polymeric materials [37]. Under the action of gamma rays and neutrons, the ionization of quartz molecules occurs in the fiber, the migration of electrons and doping impurities, the change in the density of the distribution of valence electrons, hydroxyl ions OH^- are formed from free hydrogen, and radiation absorption centers appear [36]. As a result, electromagnetic energy losses increase [35], i.e. the power of the optical signal propagating in the fiber decreases. Radiation-induced electromagnetic energy losses are determined both by the concentration of absorption centers in the matrix itself based on quartz oxide and by impurities (germanium oxide, phosphorus) [35, 36]. These losses depend on the type and energy of radiation, dose, exposure time, wavelength at which radiation-induced losses are measured, temperature, fiber type and manufacturing technology. After the end of the radiation exposure, optical fibers partially restore their original properties, in particular, an improvement in the indicators of induced electromagnetic energy losses in the optical fiber is observed, which is due to the relaxation of radiation defects [38].

It should be noted that the radiation effect is not always destructive, since it is known that special wires and cables with radiation-crosslinked polymer insulation are produced by the industry of many countries and are used in communication systems, military, aviation and space technology, electronic and computer equipment, nuclear installations, etc. [15]. At the same time, it is necessary to understand that the achievement of a positive radiation-stimulated effect occurs under a set of agreed technological conditions: dose rate, radiation temperature, cable tension force in the radiation field, etc., while under operating conditions these factors are quite random.

Special radiation-resistant optical fibers based on pure silicon oxide without impurities with a hermetic primary coating based on a highly saturated carbon varnish are being developed [39].

The operational functionality of optical fibers in onboard system cables is determined by two components: optical, which consists of the signal throughput at the appropriate distance, associated with the stability of the transmitting optical parameters, and mechanical, due to the preservation of fiber integrity. In practice, the mechanical tensile strength of an optical fiber with a diameter of 125 μm is approximately 5 GPa or 60 N for dynamic tensile strength and 3 GPa or 40 N for static tensile strength [40]. This is due to the loss of durability of optical fibers over time, which is explained by the growth of Griffiths cracks as a result of a chemical reaction under mechanical stress (stress corrosion) when the fiber breaks. Crack growth is also affected by environmental conditions, especially the humidity in which the fiber is located. In the presence of moisture, the fiber breaks even if the mechanical stress applied to it is less than the destructive one. It is static fatigue that limits the service life of the fiber [40, 41], which is a process of slow growth of micron cracks (defects) due to the

influence of moisture and tensile stresses. There is a possibility of fiber failure due to the growth of micron cracks. Moisture in the cable structure, together with the stimulated mechanical stress, causes a corrosion process at the crack tip located on the fiber surface. In this process, water molecules entering the crack from the environment activate the rupture of chemical bonds at the crack tip. This leads to an increase in the crack length under the action of the mechanical stress applied to the fiber. As the crack length increases, the stress concentration at its tip increases and the crack growth rate increases, which ultimately leads to fiber failure: the mechanical stress reaches a critical value. Therefore, the mechanical properties of optical fibers are the most important characteristics that determine the possibility of their practical use in on-board systems. To increase the mechanical strength and ensure the operational functionality of the optical fiber, special strength elements and hydrophobic materials are used in cable structures. These structural elements and materials for protecting the optical fiber from moisture are also exposed to significant influences, in particular radiation, with a change in properties, in particular mechanical. In any case, the issues of the influence of ionizing radiation not only on electrical insulating materials [27, 30, 42, 43] and optical fiber separately [34–36], but also on the cables of on-board systems in general remain unresolved. It is this approach that allows us to take into account the integral nature of the influence of complex physicochemical processes under the influence of gamma radiation on the electrical performance of electric cables and the mechanical strength of optical cables.

The goal of the work is to establish the effect of gamma radiation on unshielded cables with unshielded twisted pairs and optical cables with the determination of the dynamics of changes in the electrical properties of polyethylene insulation of conductors and the mechanical properties of aramid yarns with a waterproof coating, respectively.

Test samples of on-board system cables. Two types of cables were studied:

1. Electrical – unshielded cable with four unshielded twisted pairs of category 5e. Electrical insulation of copper conductors is made of polyethylene, protective polymer sheath – of polyvinyl chloride-based plastic. The outer diameter of the cable is 5.1 mm. The cable is designed to transmit signals in the frequency range up to 125 MHz.

2. Optical cable with single-mode optical fiber in a dense two-layer coating. The core and reflective sheath of the fiber with a diameter of 125 μm – based on quartz. Buffer primary polymer coating with a thickness of 62.5 μm – based on an ultraviolet-curing silicone varnish to ensure the mechanical integrity of the optical fiber. The second layer of the coating with a thickness of 325.5 μm is based on a thermoplastic organosilicon compound with a top layer of 15 μm of blue color. In the cable design, the power element is two strands of aramid tyarns based on Kevlar (organic fiber from the aromatic polyamide series) [44] to increase mechanical strength with a water-repellent compound applied to protect the optical fiber from moisture. The linear density of each strand of yarns is 805 tex [tex is the linear density: 1 tex = 1 g/km]. Each strand consists of 5 yarns with a linear density of 161 tex. The cable yarn is made on the basis of a polymer fire-resistant composition of orange color. The total diameter of the cable is 2.8 mm.

Table 1 shows the comparative properties of the mechanical characteristics of Kevlar® yarns manufactured by DuPont and other materials.

Table 1

Comparative analysis of mechanical and thermal properties of materials of power elements of optical cables [44]

Power element material	Density, kg/m^3	Tensile strength σ, 10^9, Pa	Young modulus E, 10^9, Pa	Relative elongation ε, %	Thermal expansion coefficient (in the longitudinal direction), 10^{-6}, K^{-1}
Kevlar 49	**1439.35**	**3.0**	**112.4**	**2.4**	**–2.2**
S-glass	2491.19	3.45	85.5	5.4	+1.7
Steel rod	7750.37	1.96	199.9	2.0	+3.7
High-strength carbon	1799.19	3.1	220.6	1.4	–0.1

The presented materials can be used as power elements of optical cables of on-board systems. Unique properties distinguish Kevlar® from other commercial artificial yarns due to the combination of high mechanical strength, high modulus of elasticity, impact strength, thermal stability with a high value of the negative coefficient of thermal expansion [44].

Thanks to the use of Kevlar yarns with a water-resistant compound, it is possible to ensure resistance to tensile forces, an optical cable of on-board systems 50 km long when the optical fiber operates at a working wavelength of 1.31 μm.

Radiation irradiation procedure. Samples in the amount of 15 segments of 5 m each from one coil of electrical and optical cables, respectively, were placed in a polyethylene container for processing in a cobalt-60 (Co^{60}) gamma radiation installation. The radiation exposure dose rate was 207 R/min. The processing time of the cable samples was determined by the absorbed dose. For each batch of 5 cable samples, the absorbed dose of gamma radiation was 100 kGy, 200 kGy and 300 kGy, respectively. The uniformity of the dose distribution when irradiating the material with gamma quanta energies of 1.17 MeV and 1.33 MeV, the radiation of which is accompanied by the decay of the Co^{60} isotope, was ensured by choosing its equivalent thickness of no more than 20 mm [45]: the diameters of the electric and optical cables do not exceed the value of the equivalent thickness.

In the initial state and after the action of irradiation, a study was conducted on the influence of radiation dose on the electrical and mechanical properties of electrical and optical cables, respectively. At all stages of the study, the cables were in an unsealed state to reduce the influence of volatile substances on the analysis results. These substances, which accumulated in the free space of the cable core, diffused out of the cables.

Numerical calculation of the electric field and capacitance of insulated conductors of an unshielded cable in a polymer protective sheath. For electrical cables, the electrical capacitance is the most sensitive electrical parameter for assessing the influence of radiation on solid polymer insulation [46], taking into account the influence of complex physicochemical processes in structural elements, including the polymer protective sheath.

The justification of the inspection scheme for monitoring the electrical capacitance of solid polymer insulation of conductors of an unshielded cable with four twisted pairs in a polymer sheath was performed on the basis of numerical modelling of a plane-parallel electrostatic field by the secondary source method [46, 47]. The method is based on the superposition of electric fields of elementary electric charges located in a vacuum.

Figure 1,*a* shows a physical model of an unshielded cable with four unshielded twisted pairs. The numbers are: from 1 to 8 – conductors, 1' – 8' – polymer insulation.

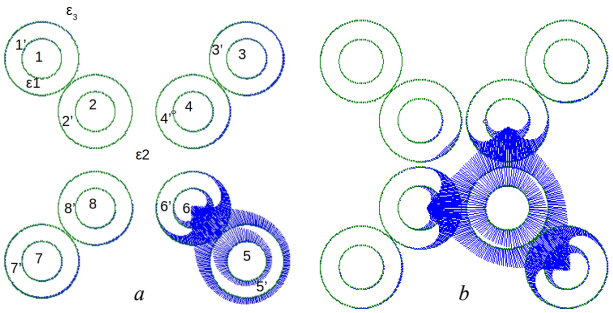

Fig. 1. Physical model of an unshielded cable with four unshielded twisted pairs (*a*) and the pattern of lines of the normal component of the intensity of the probing electric field (*b*), provided that one of the conductors is under potential and all others are at zero potential

The model neglects the helical surface of twisted pairs, which provides a plane-parallel electric field in the cable cross-section. The surfaces of conductors and conductor insulation are assumed to be circular cylindrical, which is consistent with the boundaries of the separation of media in the original problem. The difference in dielectric properties of the cable structural elements is taken into account: the dielectric permittivity of polyethylene insulation of conductors is ε_1=2.3; interphase air medium ε_2=1; protective polymer sheath ε_2=4.5. The cable is located in an air medium with dielectric permittivity ε=1.

To implement the secondary sources method, a transition is made from the calculation of the electric field in the original problem to the calculation of the electric field in a vacuum. To do this, instead of bound charges on the surfaces of the separation of the media of the original problem, free secondary electric charges are located in a vacuum (on an infinitely thin surface *S* of the same shape as the boundary of the separation of the media of the original problem).

The calculated surface density σ (C/m^2) of these secondary charges must satisfy two conditions:

1) on surfaces reflecting conductors (electrodes), the specified potentials U_i must be achieved;

2) on surfaces reflecting the boundaries of dielectric media, the condition of equality of the normal components of the electric displacement vector must be fulfilled:

$$\varepsilon_2 \cdot \left(E_n - \frac{\sigma_i}{2\varepsilon_0} \right) = \varepsilon_1 \cdot \left(E_n + \frac{\sigma_i}{2\varepsilon_0} \right), \qquad (1)$$

where E_n is the normal component of the electric field strength at point *i*, created by all charges except the one located at this point on an infinitely small surface ΔS; $\sigma_i/(2\varepsilon_0)$ is the normal component of the electric field strength at point *i*, created by the charge itself located at this point on an infinitely small surface ΔS; $\varepsilon_0 = 8.85 \cdot 10^{-12}$ F/m is the electric constant.

The first and second conditions are written as Fredholm integral equations of the first (2) and second (3) kind, respectively:

$$\frac{1}{2\pi\varepsilon_0} \int_0^L \sigma_j \cdot \ln\left(\frac{r_{0j}}{r_{ij}} \right) \cdot \mathrm{d}l_j = U_i \, ; \qquad (2)$$

$$\frac{\sigma_i}{2\varepsilon_0} - \frac{\varepsilon_2 - \varepsilon_1}{\varepsilon_2 + \varepsilon_1} \cdot \frac{1}{2\pi\varepsilon_0} \int_{S-\Delta S} \sigma_j \cdot \frac{\cos\left(\overline{r_{ij}}, \overline{n_i}\right)}{r_{ij}} \cdot \mathrm{d}l_j = 0 \, , \qquad (3)$$

where *i* is the node number where the characteristics of the electric field are sought; *j* is the node number where the charge is located; r_{ij} is the distance between points *i* and *j*; r_{0j} is the distance from point *j* to point *O*, the potential of which can be taken as zero (r_{0j} = 1 m for models whose transverse size lies in the centimeter range, which is true for the model of an unshielded cable with four twisted pairs); σ_j is the secondary charge density at point *j*; $\mathrm{d}l_j$ is the length of an infinitely small section centered at point j; $\cos\left(\overline{r_{ij}}, \overline{n_i}\right)$ is the cosine of the angle between the vectors $\overline{r_{ij}}$ and $\overline{n_i}$ – the normal vector to the interface of the media at point *i*.

Only in this case will the electric field of the calculation model be identical to the field of the original problem. The calculation of the electric field is reduced to solving a component system of linear algebraic equations (SLAE), to which (2) and (3) are reduced. Based on the numerical solution of such a SLAE, the calculated surface density (in vacuum) of secondary charges and the electric field strength are determined:

$E_i = \frac{\sigma_i}{\varepsilon_0}$ – for the surfaces of conductors (electrodes),

$E_i = \frac{\sigma_i}{2\varepsilon_0}\left(1 + \frac{1}{\alpha}\right)$ – for the interface of dielectric media (the normal component of the electric field strength from the side of the positive direction of the normal), where is the parameter associated with the dielectric permittivities of adjacent media when the normal vector is oriented from a medium with a dielectric permittivity ε_1 (polyethylene insulation) to a medium with ε_2 (interphase air medium).

The actual density σ'_i of surface charges on the surfaces of conductors insulated with a dielectric with a dielectric permittivity ε_1 is ε_1 times greater

$$\sigma' = \varepsilon_1 \cdot \sigma ,$$

which is taken into account when determining the total charge of each insulated core and electric capacitance under the condition of given potentials of the conductors.

Figures 1–4 present electric field patterns in the form of lines for the normal component of the electric field strength on the surface of conductors and the interface of dielectric media depending on the survey scheme under the condition of applying a potential of 1 V to:

- one conductor and the other seven being at zero potential (Fig. 1,*b*);
- two conductors and the other six being at zero potential (Fig. 2);
- three conductors and the other five being at zero potential (Fig. 3);
- four conductors and the other four being at zero potential (Fig. 4).

The points show the nodes on the surface of conductors (1–8) and insulation (1'–8') with the desired values of surface charge density and electric field strength in the calculation model of an unshielded cable with four unshielded twisted pairs.

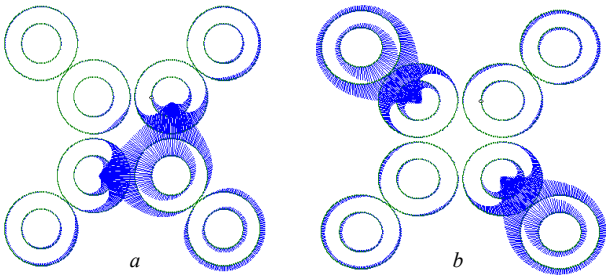

Fig. 2. Visualization of the normal component of the probing electric field strength under the condition of two insulated conductors 5 and 6 (*a*) and 1 and 6 (*b*) at a potential of 1 V

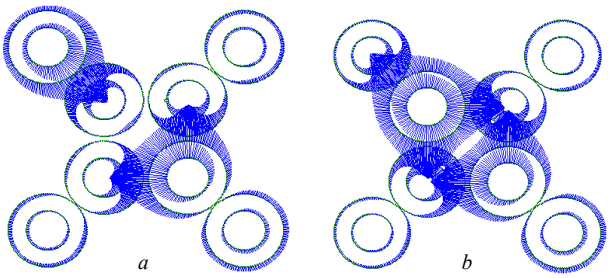

Fig. 3. Visualization of the normal component of the probing electric field strength under the condition of three insulated conductors 1, 5, and 6 (*a*) and 1 and 2, 5, and 6 (*b*) at a potential of 1 V

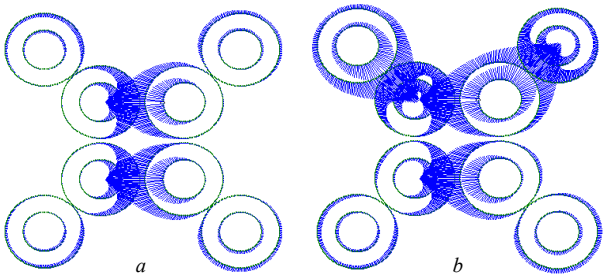

Fig. 4. Visualization of the normal component of the probing electric field strength under the condition of four insulated conductors 3, 4, 5, and 6 (*a*) and 1, 4, 6, and 7 (*b*) at a potential of 1 V

For the presented inspection schemes (Fig. 1–4), the probing electric field is concentrated both in the solid polyethylene insulation and in the interphase space of the insulated conductors, which allows determining the total C_S and partial C_{part} electric capacitances of the insulating gaps based on determining the actual density σ′ of surface charges and the total charge of each insulated conductor under the condition of a given potential.

For example, under the condition of applying a potential of 1 V to conductor 5 and zero potential to seven other conductors (Fig. 1,*a*), the partial capacitances $C_{5\text{-}1}$, $C_{5\text{-}2}$, $C_{5\text{-}3}$, $C_{5\text{-}4}$, $C_{5\text{-}6}$, $C_{5\text{-}7}$, $C_{5\text{-}8}$ of the insulating gaps between conductors 5-1, 5-2, 5-3, 5-4, 5-6, 5-7 and 5-8 are connected in parallel and determine the total capacitance C_{5S} of conductor 5:

$$C_{5S} = C_{5\text{-}1} + C_{5\text{-}2} + C_{5\text{-}3} + C_{5\text{-}4} + C_{5\text{-}6} + C_{5\text{-}7} + C_{5\text{-}8}.$$

Given that two insulated conductors 5 and 6 (Fig. 2,*a*) are under a potential of 1 V and the other 6 are under zero potential, the partial capacitances of the insulating gaps between conductors 5,6-1, 5,6-2, 5,6-3, 5,6-4, 5,6-7 and 5,6-8 are connected in parallel and determine the total capacitance of conductors 5 and 6, respectively:

$$C_{5S} + C_{6S} = C_{5,6\text{-}1} + C_{5,6\text{-}2} + C_{5,6\text{-}3} + C_{5,6\text{-}4} + C_{5,6\text{-}7} + C_{5,6\text{-}8}.$$

The inspection scheme, provided that a potential of 1 V is applied to one of the conductors and zero to the other seven, can be written in binary. For example, when conductor 5 is under a potential of 1 V, the corresponding code looks like: 00001000 (Fig. 1, *a*). For conductor 6 – 00000100 (Fig. 1, *b*).

Table 2 shows individual results of determining the electrical capacitance of conductors depending on the survey code in accordance with Fig. 1–4.

Table 2

Electrical capacitance of insulated conductors of unshielded twisted pairs of unshielded cable

Inspection code	Electrical capacitance of an insulated conductor *C*, pF/m							
	1	2	3	4	5	6	7	8
00001000	1.041	0.263	1.972	3.712	**43.13**	29.06	3.706	1.974
00000100	0.223	2.494	2.061	20.58	28.10	**76.31**	2.059	20.58
00001100	1.363	2.717	6.285	22.64	**15.26**	**48.20**	6.281	22.63
10000100	**42.21**	28.32	8.445	4.120	28.30	**42.17**	8.439	4.119
10001100	**41.95**	30.79	10.51	24.70	**47.98**	**14.11**	10.49	24.69
01001100	**29.44**	**73.55**	8.345	43.21	**15.03**	**45.71**	8.339	43.20
00111100	7.644	25.35	**8.966**	**25.56**	**8.966**	**25.56**	7.644	25.35
10010110	**39.89**	51.13	38.60	**51.16**	12.05	**27.19**	**10.72**	27.39

The difference between the total and partial capacitance values according to the 00001000 inspection scheme is 2.9 %, according to the 00001100 inspection scheme – 2.5 %.

Even with the same survey scheme, the electrical capacitances of conductors in a cable with different orientation of twisted pairs are different due to the different configuration of the electric field and the distance between insulated conductors (compare Fig. 1,*a* and Fig. 1,*b*). For an ideal calculation model of a cable with four twisted pairs twisted with the same twist steps (Fig. 1), provided that one of the conductors is under potential, and all the other seven

are under zero, there are only two schemes in which the capacitances of insulated conductors, taking into account the influence of those located nearby, differ from each other (see Table 1). The value of the electric capacitance for the inspection codes 00000100 and 00001000 differs by 76.31/43.13=1.7693 times.

For the following inspection schemes, namely: two conductors - relative to six; three conductors – relative to five; four conductors - relative to four, there are four main survey schemes. All others are inverse. Comparison of the results of numerical calculations of the electric capacitance for the main and inverse differ by 0.4 %, which indicates the high accuracy of the numerical calculation of the electric field and the determination of the electric capacitance of the conductors based on it.

In practice, four pairs of the cable are twisted with different steps to increase noise immunity when transmitting digital signals. A polymer protective sheath based on polar plastic is tightly applied to the core of the twisted pairs. This causes a more complex field configuration for any scheme of applying potential to the conductors and performing a full set of inspection schemes. First of all, to determine the dynamics of the change in electrical capacitance, i.e. the properties of the solid insulation of each conductor according to the survey scheme, each of the 8 conductors is under an applied potential – relative to all the other seven under zero potential (see Fig. 1, Table 2). In this case, the probing electric field is concentrated mainly in the solid polymer insulation of each of the 8 conductors (see Fig. 1). Such a inspection scheme provides control of the individual electrical properties of the solid polymer insulation of the conductors and should be implemented in practice. In a real cable design, with such an inspection scheme, the electrical capacitances of the conductors in the initial unirradiated state differ by no more than 4 %, which requires high accuracy of control of electrical parameters.

Dynamics of the change in electrical capacitance of insulated conductors depending on the absorbed dose of gamma radiation by cable samples. The control of the electrical capacitance of electrical cable samples in the initial state and after the absorbed radiation dose of 100, 200 and 300 kGy was carried out for four frequency values of 0.1; 1; 10 and 1000 kHz using devices with two terminals, respectively. In the frequency range from 0.1 to 10 kHz, the measurement was performed in the mode of 10-fold accumulation of results with automatic averaging to increase the control accuracy. The total number of measurements for each sample was 241 measurements before and after exposure to radiation. The measurement results of each of the five samples in the initial state and after the corresponding radiation dose were averaged.

Figure 5 shows the dynamics of the change in the electrical capacitance of insulated conductors depending on the absorbed dose of gamma radiation at different frequency values. Curves 1 correspond to the values of the capacitance of the conductors in the initial state before the action of gamma radiation. Curves 2 – at an absorbed radiation dose of 100, 200 and 300 kGy, respectively.

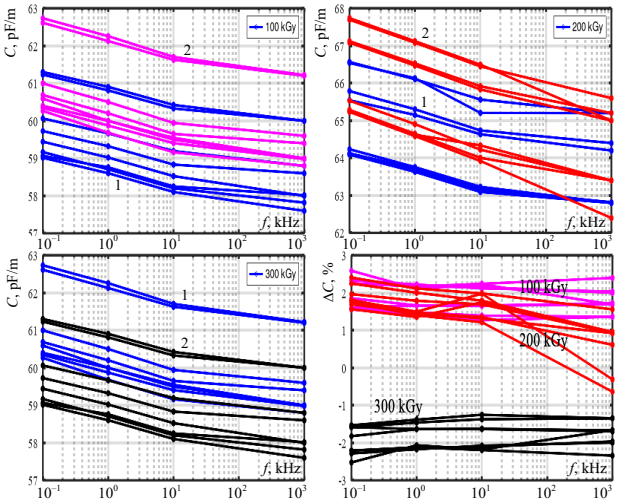

Fig. 5. Comparative analysis of the dynamics of changes in experimental frequency dependencies of electrical capacitance of polyethylene-insulated conductors before and after gamma radiation of twisted pair cable samples

Table 3 shows the determined pairwise linear correlation coefficients between the capacitance of insulated conductors of a twisted pair cable in the irradiated and non-irradiated states for different frequency values according to Fig. 5. Positive Pearson correlation coefficients indicate the presence of a significant direct relationship between the capacitance of conductors in the irradiated and non-irradiated states: the highest values at the level of 0.99 are observed in the frequency range from 0.1 kHz to 10 kHz at an irradiation dose of 200 kGy.

Table 3

Pearson pairwise correlation coefficients between the electrical capacitance of insulated conductors

Frequency, kHz			
0.1	1	100	1000
Pairwise correlation coefficient between the values of the electrical capacitance of insulated conductors in the irradiated state relative to the unirradiated state			
1-2	3-4	5-6	7-8
When exposed to gamma radiation at a dose of 100 kGy			
0.9725	0.9780	0.9705	0.9829
0.9777	0.9822	0.9755	0.9857
0.9762	0.9809	0.9740	0.9846
0.9721	0.9722	0.9653	0.9653
When exposed to gamma radiation at a dose of 200 kGy			
0.9866	**0.9858**	**0.9870**	0.9207
0.9875	**0.9866**	**0.9864**	0.9178
0.9866	**0.9861**	**0.9864**	0.9390
0.9887	**0.9877**	**0.9846**	0.9164
When exposed to gamma radiation at a dose of 300 kGy			
0.9725	0.9777	0.9762	0.9721
0.9780	0.9822	0.9809	0.9722
0.9705	0.9755	0.9740	0.9653
0.9829	0.9857	0.9846	0.9788

Figure 5 also shows the effect of radiation dose on the relative value of ΔC of the electrical capacitance in the irradiated state to the capacitance in the initial unirradiated state of cable samples (bottom figure, right). The relative value of the electrical capacitance is defined as: $(C_\gamma - C_0) / C_0 \cdot 100$, %, where C_0 is the electrical capacitance of the conductors in the initial state before the

action of gamma radiation; C_γ is the electrical capacitance of the conductors under the action of gamma radiation.

At an absorbed radiation dose of 100 kGy and 200 kGy, the relative value of the capacitance is positive, which indicates the process of crosslinking of thermoplastic polyethylene insulation. At a radiation dose of up to 100 kGy, crosslinking of polyethylene insulation occurs with the formation of cross-linking intermolecular bonds. This process causes an increase in the density of the polymer and, as a consequence, an increase in the dielectric constant, i.e. the electrical capacitance of insulated conductors. At the same time, the dispersion of the electrical capacitance – the dependence of the electrical capacitance on the frequency, which is determined by the difference in the capacitance values for the frequency of 0.1 kHz and 1 MHz, is observed to a greater extent at an absorbed dose of 200 kGy (see Fig. 5). At this radiation dose, the process of intensive destruction of the polymer insulation begins with additional crosslinking of the structure, which increases the thermal stability of the insulation [48]. Destruction leads to the formation of polymer chains of shorter length in the structure of polyethylene insulation, which causes the manifestation of the process of their polarization in the low-frequency frequency range. This corresponds to the hypothesis of the slowed-down dipole-segmental polarization of polymers, which is detected precisely in the frequency range of the experimental studies conducted. In other words, at an absorbed radiation dose of more than 200 kGy, the destruction processes dominate over the crosslinking process of polymer insulation. For a radiation dose of 300 kGy, the relative value of the capacitance changes to the opposite and becomes negative (see Fig. 5). There is a decrease in the density of polyethylene insulation and, as a result, a decrease in the capacitance of insulated conductors (see Fig. 5).

Determination of the mechanical strength of aramid yarns of an optical cable. Mechanical indicators are most suitable for assessing the effect of radiation on the protective elements of cables and are widely used, for example, in diagnosing protective sheaths of electric cables. These include the following indicators [42, 43].

1) Relative elongation at break – the main indicator of the quality of polymer insulation of cables and optical fiber. The service life of polymer insulation of cables correlates well with the value of elongation at break. The values of elongation at break are (400 – 500) % for new polyethylene insulation and only 50 % for aged: at such elongation values, the service life of polyethylene insulation is considered exhausted [49].

2) The modulus of elasticity of insulation during torsion – an indicator alternative to elongation at break.

3) The modulus of elasticity during compression. This is the simplest way to assess the condition of cable sheaths.

These indicators are not suitable for assessing the condition of power elements of optical cables due to their design.

The evaluation of the effect of gamma radiation on a power element made of Kevlar yarns impregnated with a water-repellent compound was carried out based on the determination of the mechanical tensile strength. The test was carried out in accordance with ASTM D7269/D7269M-2 «Standard Test Methods for Tensile Strength of Aramid Yarns». ASTM D7269 is an international test Standard for determining the tensile strength of aramid yarns, cords twisted from such yarns, and fabrics woven from such cords. The ASTM D7269 standard covers several variants of testing procedures for aramid yarns and Kevlar-type fibers. This test was carried out using a tensile testing machine. The machine is a mechanical-electrical integration and consists of a force sensor, a transmitter, a microprocessor and a load drive mechanism. The high-precision electronic motor can be adjusted to five speeds, and the components are connected by plugs. The breaking load measurement was performed at a constant speed of a moving clamp with a pendulum. The clamp jaws are flat with a gasket to avoid slipping and catching of the threads during the tests. The test was performed on untwisted yarns. The nominal distance between the clamps (length of the yarn samples) is 200 mm. The clamping speed is 250 mm/min. The pretension of the yarns is (20 ± 2) mN/tex. The actual breaking load at thread breakage is taken as the arithmetic mean of five test results in the unirradiated state and after each absorbed dose of radiation of the optical cable samples, respectively.

Influence of the absorbed dose of gamma radiation on the mechanical tensile strength of high-strength yarns with a waterproof compound of optical cables. The Kevlar yarns themselves demonstrate high radiation resistance under the action of accelerated electron irradiation [44]. In Fig. 6, curve 1 confirms the high mechanical properties of Kevlar® 49 yarns [44]: a slight increase of 7 % in mechanical tensile strength relative to the initial, unirradiated state is observed at an absorbed dose of up to 2000 kGy [44].

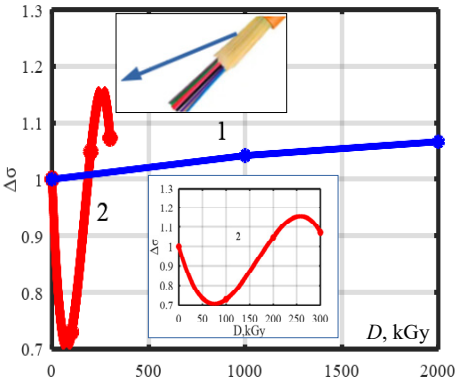

Fig. 6. Dynamics of change in mechanical tensile strength of Kevlar® 49 aramid yarns under irradiation with accelerated electrons (curve 1) [44] and of Kevlar-based aramid yarns impregnated with a water-repellent emulsion under the action of gamma radiation on optical cable samples

Irradiation of optical cable samples with Kevlar yarns impregnated with a water-repellent emulsion demonstrates a significant effect of the absorbed dose of gamma radiation on the mechanical strength of irradiated samples compared to the mechanical strength of unirradiated samples. Curve 2 in Fig. 6 corresponds to the experimental dependence of the mechanical tensile strength of high-strength Kevlar-based yarns with a

water-repellent compound, extracted from optical cable samples irradiated with a dose of 100, 200 and 300 kGy. The points on curve 2 are the result of averaging the mechanical strength values. The smooth curve 2 is a polynomial approximation of a 5th-order polynomial [50].

In the considered range of absorbed gamma radiation dose, a characteristic decrease in mechanical tensile strength by 30 % is observed at a dose of 75 kGy and an increase by 11.5 % at a dose of about 250 kGy relative to the initial unirradiated state. The decrease in mechanical strength of aramid yarns is observed due to the influence of a water-protective adsorbent. Under the influence of radiation, additional polymerization of the water-oil emulsion of polymers with ultra-high absorption capacity occurs. This leads to its shrinkage, which causes a strong effect of the influence on the mechanical strength of aramid yarns. At higher values of the absorbed radiation dose, the influence of the water-oil emulsion of polymers with ultra-high absorption capacity decreases. In this case, processes of direct influence of gamma radiation on aramid yarns with an increase in their mechanical strength are observed: the process of radiation crosslinking of organic fiber based on aromatic polyamides is traced.

Conclusions.

1. Based on numerical modeling of the electrostatic field in an unshielded electrical cable with different orientations of four unshielded twisted pairs, an inspection scheme was justified to control the individual electrical properties of solid polymer insulation of insulated conductors.

2. Experimental studies have proven the effect of an absorbed dose of 100 kGy, 200 kGy and 300 kGy of gamma radiation on the processes of crosslinking and destruction of polyethylene insulation of samples of an unshielded electrical cable. This is indirectly confirmed by the dynamics of changes in the electrical capacitance of insulated conductors of unshielded four twisted pairs according to the test scheme: each insulated conductor under potential – against all seven others under zero potential.

3. A criterion for achieving a critical state of polymer polyethylene insulation of insulated conductors under the action of gamma radiation of cables is proposed. The criterion is based on the change in the sign of the relative electrical capacitance of insulated conductors in the irradiated state to the unirradiated state of the cables of on-board systems. In the range of the absorbed dose of gamma radiation from 100 kGy to 200 kGy (in the frequency range from 0.1 kHz to 10 kHz), the relative electrical capacitance has a positive sign. At an absorbed dose of 300 kGy, it has a negative sign.

4. The synergistic effect of the influence of a water-repellent adsorbent on the mechanical strength of aramid yarns of the power element under the action of gamma radiation on samples of the optical cable of on-board systems has been experimentally proven. In the range of the absorbed dose of radiation up to 175 kGy, a decrease in the mechanical tensile strength of aramid yarns is observed, which is due to the influence of the adsorbent itself. At a gamma radiation dose of more than 175 kGy, the effect of the adsorbent decreases. The effect of radiation strengthening of the mechanical strength of aramid yarns by 11.5 % relative to the unirradiated state is observed at an absorbed dose of 250 kGy.

5. The conducted experimental studies provide grounds for increasing the radiation resistance of structural elements and the overall efficiency of the operation of electrical and optical cables of on-board systems under gamma radiation.

Conflict of interest. The authors declare no conflict of interest.

REFERENCES

1. Sahoo S., Zhao X., Kyprianidis K. A Review of Concepts, Benefits, and Challenges for Future Electrical Propulsion-Based Aircraft. Aerospace, 2020, vol. 7, no. 4, art. no. 44. doi: https://doi.org/10.3390/aerospace7040044.

2. Aretskin-Hariton E., Schnulo S.L., Hendricks E.S., Chapman J.W. Electrical Cable Design for Urban Air Mobility. *American Institute of Aeronautics and Astronautics. Aerospace Research Central.* January 2020. doi: https://doi.org/10.2514/6.2020-0014.

3. Bode I. Emergent Normativity: Communities of Practice, Technology, and Lethal Autonomous Weapon Systems. *Global Studies Quarterly*, 2024, vol. 4, no. 1, pp. 1-11. doi: https://doi.org/10.1093/isagsq/ksad073.

4. Dorczuk M. Modern weapon systems equipped with stabilization systems: division, development objectives, and research problems. *Scientific Journal of the Military University of Land Forces*, 2020, vol. 197, no. 3, pp. 651-659. doi: https://doi.org/10.5604/01.3001.0014.3959.

5. Borghei M., Ghassemi M. Insulation Materials and Systems for More- and All-Electric Aircraft: A Review Identifying Challenges and Future Research Needs. *IEEE Transactions on Transportation Electrification*, 2021, vol. 7, no. 3, pp. 1930-1953. doi: https://doi.org/10.1109/TTE.2021.3050269.

6. *Fiber Optic Cable In Military Application Market Analysis, Size, and Forecast 2025-2029: North America (US and Canada), Europe (France, Germany, Russia, UK), Middle East and Africa, APAC (China, India, Japan, South Korea), South America, and Rest of World (ROW)*. Report. 2025, 222 p. Available at: https://www.mordorintelligence.com/industry-reports/military-fibre-optic-cables-market (Accessed 27 May 2025).

7. Brunelle R., Pegge C. A history of avionic fiber optic cable development and future requirements. *IEEE Conference Avionics Fiber-Optics and Photonics*, 2005, pp. 1-2. doi: https://doi.org/10.1109/AVFOP.2005.1514127.

8. Patel H.K., Shah S.S. Detailed analysis of fiber optic networks and its benefits in defense applications. *International Journal of Advanced Research in Engineering and Technology*, 2015, vol. 6, no. 2, pp. 01-08. Available at: https://iaeme.com/Home/article_id/IJARET_06_02_001 (Accessed 27 May 2025).

9. Ruffin P.B. A review of fiber optics technology for military applications. *Proceedings of SPIE - The International Society for Optical Engineering*, 2000, vol. 10299, pp. 1-24, art. no. 1029902. doi: https://doi.org/10.1117/12.419796.

10. Kyselak M., Vavra J., Slavicek K., Grenar D., Hudcova L. Long Distance Military Fiber-Optic Polarization Sensor Improved by an Optical Amplifier. *Electronics*, 2023, vol. 12, no. 7, art. no. 1740. doi: https://doi.org/10.3390/electronics12071740.

11. Marques C., Leal-Júnior A., Kumar S. Multifunctional Integration of Optical Fibers and Nanomaterials for Aircraft Systems. *Materials*, 2023, vol. 16, no. 4, art. no. 1433. doi: https://doi.org/10.3390/ma16041433.

12. Rovera A., Tancau A., Boetti N., Dalla Vedova M.D.L., Maggiore P., Janner D. Fiber Optic Sensors for Harsh and High Radiation Environments in Aerospace Applications. *Sensors*, 2023, vol. 23, no. 5, art. no. 2512. doi: https://doi.org/10.3390/s23052512.
13. Lee H.-K., Choo J., Shin G., Kim J. Long-Reach DWDM-Passive Optical Fiber Sensor Network for Water Level Monitoring of Spent Fuel Pool in Nuclear Power Plant. *Sensors*, 2020, vol. 20, no. 15, art. no. 4218. doi: https://doi.org/10.3390/s20154218.
14. Esposito F., Stancalie A., Campopiano S., Iadicicco A. Editorial to the Special Issue Optical Fiber Sensors in Radiation Environments. *Sensors*, 2023, vol. 23, no. 22, art. no. 9117. doi: https://doi.org/10.3390/s23229117.
15. *Nexans. Nuclear industry Cable Applications. A practical guide*. 2016, 24 p.
16. Šaršounová Z., Plaček V., Prajzler V., Masopustová K., Havránek P. Influence of Optic Cable Construction Parts on Recovery Process after Gamma Irradiation. *Energies*, 2022, vol. 15, no. 2, art. no. 599. doi: https://doi.org/10.3390/en15020599.
17. Cheymol G., Maurin L., Remy L., Arounassalame V., Maskrot H., Rougeault S., Dauvois V., Le Tutour P., Huot N., Ouerdane Y., Ferdinand P. Irradiation Tests of Optical Fibers and Cables Devoted to Corium Monitoring in Case of a Severe Accident in a Nuclear Power Plant. *IEEE Transactions on Nuclear Science*, 2020, vol. 67, no. 4, pp. 669-678. doi: https://doi.org/10.1109/TNS.2020.2978795.
18. London Y., Sharma K., Diamandi H., Hen M., Bashan G., Zehavi E., Zilberman S., Berkovic G., Zentner A., Mayoni M., Stolov A., Kalina M., Kleinerman O., Shafir E., Zadok A. Opto-Mechanical Fiber Sensing of Gamma Radiation. *Journal of Lightwave Technology*, 2021, vol. 39, no. 20, pp. 6637-6645. doi: https://doi.org/10.1109/JLT.2021.3102698.
19. Francesca D.Di, Brugger M., Vecchi G.L., Girard S., Morana A., Reghioua I., Alessi A., Hoehr C., Robin T., Kadi Y. Qualification and Calibration of Single-Mode Phosphosilicate Optical Fiber for Dosimetry at CERN. *Journal of Lightwave Technology*, 2019, vol. 37, no. 18, pp. 4643-4649. doi: https://doi.org/10.1109/JLT.2019.2915510.
20. Naikwadi A.T., Sharma B.K., Bhatt K.D., Mahanwar P.A. Gamma Radiation Processed Polymeric Materials for High Performance Applications: A Review. *Frontiers in Chemistry*, 2022, vol. 10. art. no. 837111. doi: https://doi.org/10.3389/fchem.2022.837111.
21. Drobny J.G. *Radiation Technology for Polymers.* Boca Raton, CRC Press, 2021, 338 p. doi: https://doi.org/10.1201/9780429201196.
22. *Radiation Technologies and Applications in Materials Science.* Edited by Subhendu Ray Chowdhury. Boca Raton, CRC Press, 2022, 416 p. doi: https://doi.org/10.1201/9781003321910.
23. Tamada M. Radiation Processing of Polymers and Its Applications. *Radiation Applications*, 2018, pp. 63-80. doi: https://doi.org/10.1007/978-981-10-7350-2_8.
24. Ashfaq A., Clochard M.-C., Coqueret X., Dispenza C., Driscoll M.S., Ulański P., Al-Sheikhly M. Polymerization Reactions and Modifications of Polymers by Ionizing Radiation. *Polymers*, 2020, vol. 12, no. 12, art. no. 2877. doi: https://doi.org/10.3390/polym12122877.
25. Azevedo A.M.de, da Silveira P.H.P.M., Lopes T.J., da Costa O.L.B., Monteiro S.N., Veiga-Júnior V.F., Silveira P.C.R., Cardoso D.D., Figueiredo A.B.-H. da S. Ionizing Radiation and Its Effects on Thermoplastic Polymers: An Overview. *Polymers*, 2025, vol. 17, no. 8, art. no. 1110. doi: https://doi.org/10.3390/polym17081110.
26. Barlow A., Biggs J.W., Meeks L.A. Radiation processing of polyethylene. *Radiation Physics and Chemistry*, 1981, vol. 18, no. 1-2, pp. 267-280. doi: https://doi.org/10.1016/0146-5724(81)90080-7.
27. Liu B., Gao Y., Li J., Guo C., Gao J., Chen Y., Du B. Aging Behavior of Polypropylene as Cable Insulation Under Gamma-Ray Irradiation. *IEEE Transactions on Dielectrics and Electrical Insulation*, 2024, vol. 31, no. 2, pp. 956-964. doi: https://doi.org/10.1109/TDEI.2023.3337753.
28. Manas D., Ovsik M., Mizera A., Manas M., Hylova L., Bednarik M., Stanek M. The Effect of Irradiation on Mechanical and Thermal Properties of Selected Types of Polymers. *Polymers*, 2018, vol. 10, no. 2, art. no. 158. doi: https://doi.org/10.3390/polym10020158.
29. Sirin M., Zeybek M.S., Sirin K., Abali Y. Effect of gamma irradiation on the thermal and mechanical behaviour of polypropylene and polyethylene blends. *Radiation Physics and Chemistry*, 2022, vol. 194, art. no. 110034. doi: https://doi.org/10.1016/j.radphyschem.2022.110034.
30. Besprozvannykh G.V., Naboka B.G., Morozova E.V. Radiation resistance of internal cables for general industrial use. *Electrical Engineering & Electromechanics*, 2006, no. 3, pp. 82-86. (Rus).
31. Liu Z., Miyazaki Y., Hirai N., Ohki Y. Comparison of the effects of heat and gamma irradiation on the degradation of cross-linked polyethylene. *IEEJ Transactions on Electrical and Electronic Engineering*, 2020, vol. 15, no. 1, pp. 24-29. doi: https://doi.org/10.1002/tee.23023.
32. Maléchaux A., Colombani J., Amat S., Marque S.R.A., Dupuy N. Influence of Gamma Irradiation on Electric Cables Models: Study of Additive Effects by Mid-Infrared Spectroscopy. *Polymers*, 2021, vol. 13, no. 9, art. no. 1451. doi: https://doi.org/10.3390/polym13091451.
33. Li D., Sriraman A., Ni Y., Ellis I., Spencer M.P., Zwoster A., Fifield L.S. Dose Rate Effects in the Aging of Nuclear Cable Insulation Subjected to Gamma Radiation. *2022 IEEE Conference on Electrical Insulation and Dielectric Phenomena (CEIDP)*, 2022, pp. 372-375. doi: https://doi.org/10.1109/CEIDP55452.2022.9985382.
34. Girard S., Kuhnhenn J., Gusarov A., Brichard B., Van Uffelen M., Ouerdane Y., Boukenter A., Marcandella C. Radiation Effects on Silica-Based Optical Fibers: Recent Advances and Future Challenges. *IEEE Transactions on Nuclear Science*, 2013, vol. 60, no. 3, pp. 2015-2036. doi: https://doi.org/10.1109/TNS.2012.2235464.
35. Prajzler V., Masopoustova K., Sarsounova Z. Gamma radiation effects on plastic optical fibers. *Optical Fiber Technology*, 2022, vol. 72, art. no. 102995. doi: https://doi.org/10.1016/j.yofte.2022.102995.
36. Bezprozvannykh G.V., Naboka B. G., Morozova E.V. The influence of impurities on radiation-induced losses in optical fibers. *Bulletin of NTU «KhPI»*, *Series: Energy: Reliability and Energy Efficiency*, 2006, no. 7, pp. 53-58. (Rus).
37. Campanella C., De Michele V., Morana A., Mélin G., Robin T., Marin E., Ouerdane Y., Boukenter A., Girard S. Radiation Effects on Pure-Silica Multimode Optical Fibers in the Visible and Near-Infrared Domains: Influence of OH Groups. *Applied Sciences*, 2021, vol. 11, no. 7, art. no. 2991. doi: https://doi.org/10.3390/app11072991.
38. Von White II G., Tandon R., Serna L., Celina M., Bernstein R. *An Overview of Basic Radiation Effects on Polymers and Glasses*. U.S. Department of Energy, 2013, 35 p. Available at: https://www.osti.gov/servlets/purl/1671997 (Accessed 19 May 2025).
39. Bezprozvannykh G.V., Naboka B.G., Morozova E.V. Relaxation of radiation-induced losses in quartz-based optical fibers after the end of irradiation. *Bulletin of NTU «KhPI»*, *Series: Energy: Reliability and Energy Efficiency*, 2005, no. 42, pp. 57-60. (Rus).
40. Li J., Chen Q., Zhou J., Cao Z., Li T., Liu F., Yang Z., Chang S., Zhou K., Ming Y., Yan T., Zheng W. Radiation Damage Mechanisms and Research Status of Radiation-

Resistant Optical Fibers: A Review. *Sensors*, 2024, vol. 24, no. 10, art. no. 3235. doi: https://doi.org/10.3390/s24103235.
41. Bickham S.R., Glaesemann G.S., Shu Y., Scannell G.W. Reliability and Bend Loss of Optical Fibers in Tight Bend Applications. *2021 IEEE CPMT Symposium Japan (ICSJ)*, 2021, pp. 146-149. doi: https://doi.org/10.1109/ICSJ52620.2021.9648876.
42. Bezprozvannych G.V., Mirchuk I.A. Correlation between electrical and mechanical characteristics of cables with radiation-modified insulation on the basis of a halogen-free polymer composition. *Electrical Engineering & Electromechanics*, 2018, no. 4, pp. 54-57. doi: https://doi.org/10.20998/2074-272X.2018.4.09.
43. Bezprozvannych G.V., Mirchuk I.A. Influence of technological dose of irradiation on mechanical and electrical characteristics of polymeric insulation of wires. *Problems of Atomic Science and Technology*, 2018, vol. 117, no. 5, pp. 40-44.
44. *Kevlar Aramid Fiber Technical Guide. DuPont*. 2017, 24 p. Available at: https://www.dupont.com/content/dam/dupont/amer/us/en/safety/public/documents/en/Kevlar_Technical_Guide_0319.pdf (Accessed 17 May 2025).
45. Klepikov V.F., Prokhorenko E.M., Lytvynenko V.V., Zakharchenko A.A., Hazhmuradov M.A. Control of macroscopic characteristics of composite materials for radiation protection. *Problems of Atomic Science and Technology*, 2015, vol. 96, no. 2, pp. 193-196.
46. Bezprozvannych G.V., Moskvitin Y.S., Kostiukov I.O., Grechko O.M. Dielectric parameters of phase and belt paper impregnated insulation of power cables. *Electrical Engineering & Electromechanics*, 2025, no. 2, pp. 69-78. doi: https://doi.org/10.20998/2074-272X.2025.2.09.
47. Bezprozvannych G.V., Gontar Y.G., Pushkar I.A. Electrostatic field in unshielded power cables with different configurations of core. *Technical Electrodynamics*, 2025, no. 4, pp. 29-41. (Ukr). doi: https://doi.org/10.15407/techned2025.04.029.
48. Bezprozvannych G.V., Grynyshyna M.V., Kyessayev A.G., Grechko O.M. Providing technical parameters of resistive cables of the heating floor system with preservation of thermal resistance of insulation. *Electrical Engineering & Electromechanics*, 2020, no. 3, pp. 43-47. doi: https://doi.org/10.20998/2074-272X.2020.3.07.
49. Gillen K.T., Assink R.A., Bernstein R. *Final Report on Aging and Condition Monitoring of Low-Voltage Cable Materials*. Scandia National Laboratories, Nuclear Energy Plant Optimization (NEPO). SAND2005–7331, 2005. 287 p.
50. Bezprozvannykh G.V., Moskvitin Y.S. *Applied Programming in GNU Octave*. Kharkiv, NTU «KhPI» Publ., 2025. 202 p. (Ukr).

Received 18.07.2025
Accepted 20.09.2025
Published 02.01.2026

G.V. Bezprozvannych[1], *Doctor of Technical Science, Professor,*
I.A. Pushkar[2], *Deputy General Director for Production, Postgraduate Student*,
[1] National Technical University «Kharkiv Polytechnic Institute», 2, Kyrpychova Str., Kharkiv, 61002, Ukraine,
e-mail: Hanna.Bezprozvannukh@khpi.edu.ua (Corresponding Author)
[2] Scientific and Production Enterprise ALAY,
95 A2, Vidradny Ave., office 202, Kyiv, 03061, Ukraine,
e-mail: ihor.pushkar@ieee.khpi.edu.ua

How to cite this article:
Bezprozvannych G.V., Pushkar I.A. Influence of gamma radiation on the electrical and mechanical properties of on-board systems cables. *Electrical Engineering & Electromechanics*, 2026, no. 1, pp. 76-85. doi: https://doi.org/10.20998/2074-272X.2026.1.10